Exogenous 3-Iodothyronamine rescues the entorhinal cortex from β-amyloid toxicity

Alice Accorroni[1,2] PhD, MD, Grazia Rutigliano[1] MD, Martina Sabatini[3] PhD, Sabina Frascarelli[3] MS, Marco Borsò[3] MS, Elena Novelli PhD [2], Lavinia Bandini[3] MS, Sandra Ghelardoni[3] PhD, Alessandro Saba[3] PhD; Riccardo Zucchi[3] MD, PhD, Nicola Origlia[2] PhD

[1] Scuola Superiore di Studi Universitari e di Perfezionamento Sant'Anna, Pisa, Italy

[2] Institute of Neuroscience of the Italian National Research Council (CNR), Pisa, Italy.

[3] Department of Pathology, University of Pisa, Pisa, Italy.

email addresses of authors: accorroni.alice@gmail.com (AA), grazia.rutigliano.gr@gmail.com (GR), marti.saba88@gmail.com (MS), s.frascarelli@yahoo.it (SF), marco.borso@student.unisi.it (MB), novelli@in.cnr.it (EN), lavinia.bandini@student.unisi.it (LB), sandra.ghelardoni@med.unipi.it (SG), alessandro.saba@med.unipi.it (AS), riccardo.zucchi@med.unipi.it (RZ), origlia@in.cnr.it (NO).

Running title: T_1AM counteracts β-amyloid toxicity

Key words: 3-iodothyronamine, trace amine-associated receptor 1, β-amyloid, brain, Alzheimer's disease

Abstract

Background. A novel branch of thyroid hormone (TH) signaling is represented by 3-iodothyronamine (T_1AM), an endogenous TH derivative that interacts with specific molecular targets, including trace amine associated receptor-1 ($TAAR_1$), and induces pro-learning and anti-amnestic effects in mice. Dysregulation of TH signaling has long been hypothesized to play a role in Alzheimer's disease (AD). In the present investigation, we explored the neuroprotective role of T_1AM in beta amyloid (Aβ)-induced synaptic and behavioral impairment, focusing our study on the entorhinal cortex (EC), an area which is early affected by AD pathology.

Methods. Field potentials were evoked in EC layer II and long-term potentiation (LTP) was elicited by high frequency stimulation (HFS). T_1AM (5 μM) and/or $Aβ_{142}$ (200 nM), were administered for 10 minutes, starting 5 minutes before HFS. Selective $TAAR_1$ agonist RO5166017 (250 nM) and $TAAR_1$ antagonist EPPTB (5 nM) were also used. The electrophysiological experiments were repeated in EC-slices taken from a mouse model of AD (mhAPP, J20 line). We also assessed the *in vivo* effects of T_1AM on EC-dependent associative memory deficits, that were detected in mhAPP mice by behavioral evaluations based on the novel-object recognition paradigm. $TAAR_1$ expression was determined by Western blot, while T_1AM and its metabolite 3-iodothyroacetic acid (TA_1) were assayed by HPLC coupled to mass spectrometry.

Results. We demonstrated the presence of endogenous T_1AM and $TAAR_1$ in the EC of wild type and mhAPP mice. Exposure to Aβ (1-42) inhibited LTP, and T_1AM perfusion (at a concentration of 5 μM, leading to an actual concentration in the perfusion buffer ranging from 44 to 298 nM) restored it, whereas equimolar T_3 and TA_1 were ineffective. The response to T_1AM was abolished by $TAAR_1$ antagonist EPPTB, while it was mimicked by $TAAR_1$ agonist RO5166017. In the EC of APPJ20 mice, LTP could not be elicited, but it was rescued by T1AM. The i.c.v. administration of T1AM (0.89 μg/Kg) also restored recognition memory that was impaired in mhAPP mice.

50 Conclusions. Our results suggest that T_1AM and $TAAR_1$ are part of an endogenous system that can

51 be modulated to prevent synaptic and behavioral deficits associated with Aβ-related toxicity**.**

Introduction

Thyroid hormones (TH) have an established role in the development of the central nervous system (1), and may also play a role in dementia and in Alzheimer's disease (AD) (2-7). Animal studies have supported a role of TH as neuroprotective agents in brain areas that are early affected in AD. Indeed, TH administration was shown to reduce hippocampal neuronal damage induced by ischemia and to protect neurons from glutamate-induced death (8, 9). Whereas, hypothyroidism reduced hippocampal neurogenesis (10) and in CA1 neurons it impaired long-term potentiation (LTP), that was then restored by TH administration (11, 12). Moreover, TH have been demonstrated to influence amyloid precursor protein (APP) transcription, the alternative splicing of APP mRNA, APP protein processing (13-15) and to rescue memory deficits in AD rodent models (16-19). These results suggest that TH may exert a neuroprotective role against β-amyloid (Aβ)-dependent neuronal impairment, which is assumed to be one of the pathophysiological mechanisms involved in AD.

In recent years, the picture of TH signaling has grown more complex than originally believed. While the canonical concept holds that TH receptors behave as ligand-dependent transcription factors, the relevance of non canonical actions has been recognized (20). Another significant breakthrough has been the discovery of novel TH derivatives acting on receptors that differ from nuclear TH ones. In particular, 3-iodothyronamine (T_1AM), allegedly derived from TH through decarboxylation and deiodination, has been reported to be a chemical messenger that activates a G protein-coupled receptor known as trace amine-associated receptor 1 ($TAAR_1$) with high potency (21). $TAAR_1$ is widely expressed in the brain (22, 23), it has been implicated in several neuropsychiatric disorders and has attracted attention for being a potential drug target (24-26). The intra-cerebro-ventricular (i.c.v.) administration of T_1AM in mice produced a pro-learning and

anti-amnestic response (27, 28). Furthermore, it has been suggested that some of T_1AM effects could be due to its oxidative product, 3-iodotyhyroacetic acid (TA1) (28-30).

In the present work, we aimed at determining whether T_1AM may play a protective role in a specific model of neuronal injury, namely Aβ-dependent synaptic and behavioral impairment. We focused our study on the layer II of the entorhinal cortex (EC), an area that is early affected in AD (31, 32). The rationale for this choice is also related to previous observations showing that EC horizontal connections are vulnerable to the effects of exogenously applied Aβ(1-42) oligomers (33, 34). Moreover, in previously published projects, we showed that EC synaptic function is early affected in mutant human APP transgenic mice (mhAPP, J20 line), and that the synaptic dysfunction is associated with an impairment of specific forms of associative memory (35), which depend on EC functional integrity (36, 37).

Our results show that exogenous T_1AM is able to rescue the EC in both models of Aβ-toxicity. This finding adds a novel issue to the discussions on the elusive links between TH signaling, Aβ effects and the pathophysiology of AD.

Materials and Methods

Animals. Transgenic mhAPP mice (APPsweInd, line J20) overexpressing an alternatively spliced human APP minigene that encodes hAPP695, hAPP751, and hAPP770, bearing mutations linked to familial AD (38) were used, together with their littermate controls (C57BL/6J). All experiments were conducted in male mice at the age of 2 months, in accordance with the Italian Ministry of Health and the European Community guidelines (Legislative Decree n. 116/92 and European Directive 86/609/EEC). The experimental protocol (IACUC document) was approved by the Ministry of Health (protocol n. 192/2000-A). Two-month-old TAAR1 knockout mice (KO) (C57BL/6J × 129 Sv/J) and wild type (WT) littermates were generously provided by Stefano Espinoza (Istituto Italiano di Tecnologia, Genova, Italy).

Drugs. T_1AM and 3-iodothyroacetic acid (TA1) were synthesized as described previously (39) and were generously provided by Dr. Thomas Scanlan (Oregon Health & Science University); 3,5,3'-triiodo-L-thyronine (T3) and $TAAR_1$ antagonist EPPTB were purchased from Sigma-Aldrich (St.Louis, MO); the $TAAR_1$ agonist RO-5166017 was generously provided by Dr. Raul Gainetdinov (University of St. Petersburg). Aβ(1-42) was purchased from Abbiotec. Oligomeric Aβ(1-42) peptide was prepared as described previously and characterized by atomic force microscopy (40) and mass spectrometry (41). Aliquots were stored at -20°C in DMSO as a 200 mM stock solution and diluted to the desired final concentration in artificial CSF (ACSF), containing the following (in mM): 119 NaCl, 2.5 KCl, 2 $CaCl_2$, 1.2 $MgSO_4$, 1 NaH_2PO_4, 6.2 $NaHCO_3$, 10 HEPES, 11 glucose.

In vitro Electrophysiology. Electrophysiology was performed as in Origlia et al. (33, 34, 41). Briefly, mice were anesthetized with urethane i.p. injections (20% sol., 0.1 ml/100 g body weight) and then decapitated. Horizontal EC-hippocampal slices were produced using a vibratome (Leica

VT1200S). All steps were performed in ice cold oxygenated ACSF. Slices were then transferred to a chamber and perfused at a 2-3 ml/min rate. Field potentials (FPs) were evoked by a concentric bipolar stimulating electrode in the layer II of EC. Basal recording was carried out using stimulus intensity evoking a response whose amplitude was 50–60% of the maximal amplitude. After 15 min of stable baseline, LTP was induced by high frequency stimulation (HFS, three trains of 100 pulses at 100 Hz, 10 s interval). After HFS, FPs were monitored every 20 s for at least 40 min. The magnitude of LTP was calculated as the average of the relative amplitudes (compared to baseline) of FPs recorded in the last 10 min. Values were expressed as percentage change relative to the baseline. Data collection and analysis were performed blindly by two different operators. Aβ (200 nM), T_1AM (5 µM), $TAAR_1$ antagonist EPPTB (5 nM) and $TAAR_1$ agonist RO5166017 (250 nM) were added to ACSF perfusion and administered for 10 minutes, 5 minutes before and 5 minutes after HFS.

I.c.v. injection. Drug administration was performed under avertin-induced anesthesia according to the method described by (27, 42), with minor modifications. The depth of anesthesia was checked by monitoring the respiratory rate (reduced within 2 min) and testing for lack of a pain response to gentle pressure on the hind paws. The head of the anaesthetized mouse was positioned into a stereotaxic system and firmly blocked. A fine needle was inserted perpendicularly through the skull into the brain at the coordinates of one of the lateral ventricles, identified according to the Atlas of mouse brain (y: -0.3 mm / x: -1 mm / z: -1,5 mm). Ten µL was then slowly injected (in 20 s) into a lateral ventricle as per the protocol described by Manni et al (27). Immediately after needle removal, the animal remained quiet for approximately 1 min and then resumed its normal activity.

Behavioral study. Behavioral testing was performed as described in (37). To habituate the mice to the experimenter, they underwent extensive handling for one week before the experiments. Behavioral testing proceeded in two stages: habituation and performance of specific tasks that included novel object-place recognition task (in OPRT) and novel object-place-context recognition task (in OPCRT), as described in Wilson et al (37). Habituation and testing took place in a 60-cm square box (arena) with 40-cm high walls that could be shaped with two sets of contextual features (to be used in the OPCRT). The objects were easily cleanable household objects approximately the same size as a mouse in at least one dimension, and made from plastic, metal or glass. During the habituation phase, the mice were exposed to the arena for one hour for 3 consecutive days before the test. Vehicle or T_1AM were injected i.c.v. on the 3rd day, then OPRT and OPRCT took place 1 hour after the recovery from i.c.v. injections.

Object exploration was monitored via an overhead camera. Exploration time was defined as the time spent in the object close proximity (within 2 cm), with the nose directed towards it, or sniffing/touching the object with the nose. Exploration time did not include the periods in which the mice were pointing their nose away from the object, even if they were beside the object, running around it, or climbing on it. To check for reliability, each observer re-scored a subset of videos in a blind fashion for each task and these scores were found to be consistent (within 10%). To determine the relative exploration of novel and familiar objects, observation scores were converted into discrimination indices (DI) according to the formula:

$$DI = \frac{time\ at\ novel\ object - time\ at\ familiar\ object}{time\ at\ novel\ object + time\ at\ familiar\ object}$$

To control for differences in locomotion and to assess anxious behavior, the Open Field Test was also performed in the same arena used for the behavioral testing. We used the open-source toolbox developed by Patel et al. (43) to automatically compute the total ambulatory distance as well as the amount of time spent in outer zones versus inner zones (40x40).

Analysis of T_1AM and TA_1.

T_1AM and its metabolites (namely TA_1, thyronamine and thyroacetic acid) were assayed as previously described (27, 44), with minor changes. Instrument layout consisted in an Agilent (Santa Clara, CA, USA) 1290 UHPLC system, including a binary pump, a column oven, and a thermostatic autosampler, coupled to an AB-Sciex (Concord, Ontario, Canada) API 4000 triple quadrupole mass spectrometer, equipped with Turbo-V IonSpray source. HPLC separation was carried out by a 2x50 mm, 3 µm particle size, Gemini C18 column (Phenomenex, Torrance, CA), protected by a Phenomenex Security Guard Cartridge Gemini C18 and maintained at 20 °C in the column oven. The mobile phase included methanol/acetonitrile (1:4 by volume) containing 0.1% formic acid (solvent A) and water containing 0.1% formic acid (Solvent B). Flow rate was 300 µl/min and gradient conditions were as follows: 3 min 5% A (equilibration time), 4.5 min from 5 to 90% A, 0.5 min 90% A; 2.5 min from 90 to 100% A.

Mass spectrometry acquisitions were carried out by a selected reaction monitoring (SRM) based method operating either in positive ion mode or negative ion mode, for T_1AM and TA_1 , respectively. Three transitions were monitored for each compound (*m/z*: T_1AM 356.2 $\rightarrow$ 195.2, 356.2 $\rightarrow$ 212.2, 356.2 $\rightarrow$ 339.1; T_1AM -D4 360.2 $\rightarrow$ 199.2, 360.2 $\rightarrow$ 216.2, 360.2 $\rightarrow$ 343.1; TA_1 369.1 $\rightarrow$ 127.2, 369.1 $\rightarrow$ 197.1, 369.1 $\rightarrow$ 325.3; TA_1-D4 373.1 $\rightarrow$ 127.2, 373.1 $\rightarrow$ 200.1, 373.1 $\rightarrow$ 329.3), making use of optimized declustering potentials (DPs), collision energies (CEs), and collision exit potentials (CXPs). Further operative parameters were set as follows: IonSpray Voltage (ISV), 5.0 and -4.2 kV; Gas Source 1 (GS1), 70; Gas Source 2 (GS2), 55; turbo temperature (TEM), 650 °C; entrance potential (EP), 10 V; collision (CAD) gas, nitrogen; operative pressure with CAD gas on 3.9 mPa. Calibration curves ranged from 0.25 to 100 ng/ml for T_1AM and from 0.50 to 200 ng/ml for TA_1.

When ACSF was assayed, each sample (0.1 mL) was spiked with 10 µL of a suitable mixture of internal standards (16 pmol of T_1AM-D_4 and 21 pmol of TA_1-D_4). Methanol (0.4mL) was then added and samples were shaken for 10 minutes. After centrifugation at 22780 x g for 10 min, the supernatant was dried, reconstituted with water/methanol (70/30 by volume), and injected into the LC-MS-MS system. EC slices were homogenized and extracted as described by (45).

$TAAR_1$ analysis in EC slices. EC slices were fixed in 4% paraformaldehyde for 3 h immediately after the experiment, then cryoprotected in 30% sucrose PBS solution and finally cut at 25 µm thickness using a cryostate. Slices were washed three times in PBS, treated with a solution containing 0.5% Triton X-100, 5% BSA 5% and 10% horse serum, and then incubated with mouse anti NeuN antibody (Millipore, 1:50) overnight at 4°C. The sections were subsequently washed in 0.3% Triton X-100 in PBS and incubated with a rabbit anti-$TAAR_1$ polyclonal antibody (Abnova, dilution 1:500) for 3 hours at room temperature. After washing, secondary antibodies were added, namely anti-rabbit IgG Rhodamine Red X conjugated (Jakson Immunoresearch) and anti-mouse IgG conjugated with Alexa Fluor 488 (Molecular Probes) at 1:1000 dilution in 1% BSA-PBS for 3 h at room temperature, washed 3 × 10 min in PBS and cover slipped with Vectashield (Vector Laboratories). Serial optical sections were acquired using an Axio Imager Z2 microscope (Carl Zeiss) and multi-channel images (transmitted fluorescence) were produced with ApoTome 2. High resolution images were obtained using EC Plan-NEOFLUAR 20× /0.5 and 40x /1.25 objectives. Analysis of TAAR1 immunofluorescence signal was performed offline on TIFF images using MetaMorphR 5.0 r1 (Universal Imaging, Inc., Downingtown, PA, USA). The average fluorescent staining was calculated for each image using the quantification tool based on the detection of the contrast threshold. Three measures were obtained for each image and expressed as percentage of the area over the threshold.

For Western blot, EC slices were homogenized in a lysis buffer (10 mM Tris, pH 7.6, 100 mM NaCl, 1% Triton X-100, 0.1% SDS) containing protease and phosphatase inhibitors (2mM Na_3VO_4, 1 mM NaF, 20 mM $Na_4P_2O_7$) and centrifuged at 13,000 rpm for 10 minutes at 4°C. An equal amount of proteins (50 µg) were resolved electrophoretically on a 12% Bis-Tris gel (Bio-Rad Criterion XT). Proteins were transferred onto a polyvinylidene difluoride membrane (0.45 µm), and blocked for 1 hour at room temperature in Odyssey blocking buffer (LI-COR, Biosciences). To evaluate the presence of $TAAR_1$, membranes were probed with primary antibodies against $TAAR_1$ (Abcam, 1 : dilution 1:1000), at 4°C overnight in a solution of Odyssey blocking buffer and PBS with 0.2% Tween-20 (1:1). After washing, the membranes were incubated with anti-rabbit IRDye 800CW secondary antibody (926-32211, LI-COR Biosciences) for 1 hour at room temperature in a solution of Odyssey blocking buffer and PBS with 0.2% Tween-20 (1:1). β-Tubulin (#2128, CellSignaling) was used as house-keeping protein. Blots were imaged with an LI-COR infrared imaging system (OdysseyCLx, LI-COR Biosciences), and densitometry analyses were performed using Image Studio Lite v4.0software (LI-CORBiosciences).

Statistical analysis. Data are reported as mean±SEM. In electrophysiological experiments, comparisons between experimental groups or between FP amplitudes at different time points were performed by two-way repeated-measures ANOVA with pair wise multiple comparison procedures (Holm–Sidak method, Sigmaplot 12.0). In the other experiments, one-way ANOVA was applied. One-sample t tests was used to determine whether the discrimination index was different from zero in the behavioral tests. Differences were considered as significant when $p < 0.05$.

Results

$TAAR_1$ and T_1AM are present in the entorhinal cortex

Western blot analysis showed $TAAR_1$ expression in the EC, both in WT and mhAPP mice, with no significant difference in signal intensity between the two groups (Figure 1A-B). Co-localization of $TAAR_1$ with the neuronal marker NeuN was observed by double immunostaining, both in mhAPP and in WT EC slices (Figure 1C). Quantification of immunofluorescent staining did not reveal any significant difference between WT and mhAPP mice (Figure 1D). Representative LC-MS/MS chromatograms of EC homogenate are shown in Figure 2A. A clear T_1AM signal was apparent, as shown by the presence of all transitions with appropriate ratios. The endogenous T_1AM concentrations we measured in our sample were in the order of a few pmoles per g of wet tissue, and the difference between WT and mhAPP mice did not reach statistical significance (5.71±0.78 vs. 4.39±0.1 pmol/g, p= 0.072; Figure 2B).

T_1AM acute perfusion counteracts Aβ-induced inhibition of LTP

We focused our studies on the EC, one of the earliest affected brain regions in AD and a cortical area whose synaptic activity is negatively affected by Aβ (1-42). As reported in Figure 3A, we observed that T_1AM, at concentration up to 5 µM, did not alter the input–output curve with respect to vehicle-treated slices. The same concentration of T_1AM was applied to EC slices for 10 min, starting 5 min before HFS delivery, and we did not observe any significant change in the magnitude of LTP (130 ± 8% vs. 132±6% of baseline; Figure 3B). Then we tested whether 5 µM T_1AM could rescue LTP in EC slices treated with 200 nM oligomeric Aβ(1-42). Indeed, this was the case as a statistically significant difference between groups (p = 0.004) was observed (Figure 3C). In line with previous reports (33), Aβ(1-42) administration inhibited LTP, whereas, the co-administration of T_1AM restored it. In fact, the mean LTP was significantly higher in slices perfused

255 with T_1AM and Aβ(1-42) with respect to slices treated with Aβ(1-42) alone (127±8% vs. 104±2% of
256 baseline, p = 0.001) and was comparable to that observed in vehicle treated slices. As a control
257 experiment, we also investigated the effect of T_3, the classical TH and putative T_1AM precursor.
258 Acute perfusion with T_3 (5 μM) had no effect on basic synaptic transmission and LTP expression
259 (Figure 3 A-B), and, when T_3 was co-administered with Aβ, it did not revert Aβ-induced synaptic
260 plasticity impairment (Figure 3C).

261 Due to the complexity of protein binding, cellular uptake and tissue metabolism (46),
262 nominal T_1AM concentration does not necessarily reflect the concentration achieved at receptor
263 level. To get a better estimate of the latter, in parallel experiments, we assayed T_1AM and its
264 metabolites (namely: TA_1, thyronamine, and thyroacetic acid) in the perfusion buffer eluted from
265 EC slices, which is usually assumed to be in equilibrium with the extracellular fluid. As shown in
266 Figure 4A, during T_1AM infusion its concentration (averaged over 5-15 min periods) ranged from
267 107±2 to 298±39 nmol/l, and decreased in the washout phase, reaching 44±10 nmol/l in the 40-55
268 min interval. Among T_1AM metabolites, only TA_1 was detected. Its concentration peaked at
269 198±51 nmol/l and decreased to 137±22 nmol/l at the end of the washout phase. Thus, exogenous
270 T_1AM was taken up and transformed into its main metabolite during the experiment.

271 Since TA_1 has been suggested to mediate some neurological effects induced by T_1AM
272 administration (28), and to have neuroprotective properties in a model of kainate toxicity (47), we
273 tested the effect of 5 μM TA_1 on Aβ-induced inhibition of LTP in the EC (Figure 4B). Like T_1AM, TA_1
274 did not affect LTP in EC slices. However, in contrast to T_1AM, we observed that TA_1 administration
275 did not rescue LTP in EC slices after exposure to Aβ (mean FPs amplitude was 96±6 % of baseline
276 vs. 122±6 % in slices treated with TA_1 alone, p=0.035).

277

278 **$TAAR_1$ contributes to the protective effects of T_1AM against Aβ-induced toxicity**

T_1AM is known to be a high affinity agonist of $TAAR_1$ (EC_{50} = 112 nM in the mouse), however, it also has additional molecular targets, including other aminergic receptors, transient receptor potential channels, and membrane transporters (46, 48). To determine whether $TAAR_1$ mediates T_1AM-induced rescue of synaptic dysfunction, we used a selective antagonist (EPPTB) and a selective agonist (RO5166017) of $TAAR_1$. EPPTB was used at a concentration that was demonstrated not to modify LTP magnitude in control experiments (5 nM) (Figure 5A). When T_1AM (5 µM) was co-perfused with EPPTB in the presence of Aβ, LTP was not rescued (99±6 % vs 102±3% with vehicle + Aβ and 129±8 % with T_1AM + Aβ, p = 0.001), although EPPTB alone did not modify the response to Aβ (Figure 5B). Then, we assessed the effects of RO5166017, a synthetic high-affinity high-selectivity $TAAR_1$ agonist (24). The perfusion of WT EC slices with 250 nM RO5166017 did not induce a significant change in LTP expression (Figure 5A), but the application of 250 nM RO5166017 restored LTP in Aβ treated slices, indeed LTP magnitude in RO5166017-treated EC slices was significantly different from that recorded in slices perfused with Aβ alone (141±8% vs. 105±2%, p =0.002). As observed in the case of T_1AM, the response to RO5166017 was prevented by EPPTB co-perfusion (Figure 5C). We also had the opportunity to access a few TAAR1 KO mice, and we performed *ex vivo* electrophysiological recordings from the same circuitry evaluated in the previous experiments. As shown in Figure 6, LTP was significantly impaired in EC slices taken from TAAR1 KO mice compared to control mice (n=3). These results are consistent with the hypothesis that $TAAR_1$ mediates T_1AM effects on Aβ-induced impairment of LTP, and that the T_1AM- $TAAR_1$ system may represent a new signaling pathway that rescues LTP after exposure to Aβ.

T_1AM counteracts early synaptic plasticity impairment in mhAPP mice

The above results prompted us to extend the investigation on the protective role of T_1AM and $TAAR_1$ to a mouse model characterized by progressive accumulation of Aβ. Specifically, we used the AD transgenic mouse model (mhAPP, J20-line), overexpressing human APP bearing mutations linked to familial AD (49). We tested the hypothesis that T_1AM could rescue LTP expression, that in this model is impaired in EC since 2 months of age (35).

FPs recordings confirmed that HFS of the EC layer II did not induce LTP in slices taken from 2-month old mhAPP mice (mean amplitude 100±4 % of baseline; Figure 7A) and that T_1AM (5 μM) perfusion rescued LTP (120±4 % of baseline, p = 0.001 *vs*. vehicle treated mhAPP; Figure 7A). Furthermore, T_1AM effect was inhibited in co-perfusion with $TAAR_1$ antagonist EPPTB (5 nM) (90 ± 5 % of baseline), while a significant rescue of LTP was also achieved by perfusion with the $TAAR_1$ agonist RO5166017 (118±4 % of baseline, p = 0.026; Figure 7B). These findings are in line with the results observed in WT slices exposed to exogenous Aβ, and suggest that in the presence of APP overexpression, acute T_1AM application rescues synaptic plasticity through $TAAR_1$ activation.

Intracerebroventricular injection of T_1AM ameliorates early EC-dependent behavioral impairment in mhAPP mice

Our electrophysiological findings encouraged us to explore the neuroprotective effect of T_1AM *in vivo*. Our aim was to investigate whether the acute i.c.v. administration of T_1AM in mhAPP mice could restore mice ability to perform EC-dependent behavioral tasks. As a matter of fact, the lateral EC is required for associative memory tasks based on the combined elaboration of both spatial and non-spatial information (i.e. referred to contexts and object position). Spatial associative memory can be assessed with different behavioral tests that include OPRT and OPCRT, which are selectively affected by synaptic deficits in the lateral EC, e.g. those produced by progressive accumulation of Aβ in mhAPP mice (35, 37).

As reported in Figure 8A, no difference was found between experimental groups with regard to locomotor activity and exploration; indeed, the total distance covered during the exploration of the arena in the open field test and the time spent in exploring the center of the arena during the trials (Figure 8B) were comparable in the different experimental groups. In the OPRT and OPCRT tasks, a statistically significant difference between groups was observed (OPRT, $p = 0.003$; OPCRT, $p = 0.001$). As reported in Figure 8C and D, the performance of vehicle-injected mhAPP mice revealed an impairment in the ability to discriminate the novel object in relation to both its position and the surrounding context. The average DIs for mhAPP mice were not significantly different with respect to what can be expected by chance for both OPRT and OPCRT (0.02± 0.02 and 0.00 ± 0.03; Figure 8C and 8D) and they were significantly different from DIs of age-matched WT mice ($p < 0.01$ for OPRT and OPCRT respectively).

In line with our electrophysiological findings, i.c.v. treatment with T_1AM (0.89 μg/Kg) ameliorated behavioral impairment in mhAPP mice, as mice showed a preference toward novelty not only in OPRT but also in the more complex OPCRT version of the task (Figure 8C and 8D). The DIs in OPRT and OPCRT calculated for mhAPP mice treated with T_1AM were significantly greater than chance (0.21±0.05 and 0.32±0.08, $p=0.004$ and $p=0.002$ respectively) and significantly different from those obtained for vehicle-treated mhAPP mice ($p = 0.02$ and $p < 0.01$ for OPRT and OPCRT respectively), while they were comparable to those calculated for WT mice (averaging 0.24±0.05 and 0.35±0.02, respectively). As a control experiment, a group of WT mice was injected with T_1AM and no significant difference was found between this group and WT vehicle injected mice both in the OPRT and in OPCRT (0.27±0.05 and 0.30±0.01). Altogether these results indicate that T_1AM i.c.v. administration ameliorates behavioral performance in mhAPP mice without any effect on locomotor activity and exploration.

Discussion

A novel insight in the complexity of TH signaling was provided by the discovery that TH derivatives represent additional chemical messengers. In particular, T_1AM has been detected in rodent brain (21, 44) and its administration in mice produced relevant neurological effects that are partly synergic to those induced by TH (50). Furthermore, T_1AM has been proposed as a memory enhancer as it induced pro-learning and anti-amnestic effects in mice (27, 28).

We investigated the effects of T_1AM on the early signs of neurodegeneration in models of Aβ toxicity, focusing our study on EC layer II. This EC layer is one of the earliest affected brain regions in AD pathology (31) and it also represents the origin of the perforant pathway, a connection that shows significant synapse loss in the early phases of AD (51, 52). Furthermore, previous studies have demonstrated a particular vulnerability of the EC to the effects of exogenously applied oligomeric Aβ(1-42) (33, 34), and early EC synaptic dysfunction has been described in a mouse model characterized by progressive accumulation of human Aβ (35).

In this study, we showed that T_1AM and its receptor $TAAR_1$ are present in the EC of WT and mhAPP mice. Then, we demonstrated that T_1AM counteracts Aβ-induced inhibition of LTP at the level of EC layer II, both when Aβ is acutely administered (Aβ 1-42 oligomers) and when it accumulates endogenously (mhAPP mice). Regarding the possible mechanism of action, T_1AM interacts with different cellular targets including $TAAR_1$, other TAAR subtypes, monoamine transporters, adrenergic receptors, transient receptor potential channels (53-55). T_1AM shows the highest affinity for $TAAR_1$ (EC50=112 nM in mice) (21), which has been implicated in several neuropsychiatric disorders and whose activation induced pro-cognitive effects in rodent and primate models (24, 56). In the present investigation, the response to RO5166017 (a selective $TAAR_1$ agonist) and EPPTB (a selective $TAAR_1$ antagonist) strongly suggests that the effects

produced by T_1AM on LTP are mediated by $TAAR_1$, although we cannot formally exclude the possible involvement of other receptors.

To get further insight into the response to T_1AM, we estimated the local concentrations of this messenger after exogenous administration. In particular, we assayed T_1AM and its main metabolites in the ACSF eluted from EC slices, which is assumed to be in equilibrium with the extracellular space. During the electrophysiological recording, T_1AM concentration was in the range of 40-300 nmol/l, i.e. in the same order of magnitude of the functional EC_{50} measured when vertebrate $TAAR_1$ was expressed in heterologous cells (57). This is about one order of magnitude higher than the endogenous concentration detected in crude brain homogenate (27-29, 44). However, the technical problems associated with T_1AM assay in biological matrices (58), and the lack of knowledge about cellular and subcellular T_1AM distribution, make it difficult to compare these results. Further experiments will be necessary to determine the potential physiological or pathophysiological role of $T_1AM/TAAR_1$ signalling in the brain.

Interestingly, very low (picomolar) concentrations of Aβ have been reported to favor LTP in hippocampus (59), although higher concentrations are detrimental for synaptic plasticity, as confirmed by our investigation in the EC. Therefore, it is not excluded that the $T_1AM/TAAR_1$ system may play a modulatory role on the response of LTP to the availability of Aβ, either under physiological conditions or in disease.

An initial approach to the evaluation of this hypothesis may be represented by the analysis of $TAAR_1$ KO mice. While they appear grossly normal, a neurological phenotype is actually present in homozygotes (reviewed in ref. (23)). Much interest has been raised by behavioral and electrophysiological observations, which suggest increased dopaminergic drive, pointing to a putative cross-talk between $TAAR_1$ and the dopaminergic system. However, subtle evidence of cognitive dysfunction has also been reported, and transgenic mice appeared to be slower in

learning how to perform cognitive tests (56). Consistent with a potential physiological role of $TAAR_1$ in memory and cognition, in a limited number of experiments performed on EC slices obtained from $TAAR_1$ KO mice we observed a significant impairment of LTP vs WT littermates. However, it is important to point out that these findings are preliminary and further evaluations will be needed to confirm the involvement of TAAR1 in LTP.

It is interesting to observe that our experiments showed a trend towards a reduction in endogenous T_1AM concentration and in $TAAR_1$ expression in mhAPP mice (Figure 1B and Figure 2B). The possibility of a downregulation of the endogenous $T_1AM/TAAR_1$ system in this experimental model is intriguing, and it might open new pathophysiological hypotheses. However, the number of mHAPP samples available was limited and statistical significance was not achieved, so further experimental work is needed to determine whether changes in this system really occur in this transgenic model.

Notably, T_1AM levels in the eluate were about 16-125 fold lower than the administered dose, suggesting significant tissue metabolism and/or uptake. TA_1 was the only metabolite that we could detect. Indeed, the kinetic of TA_1 release was consistent with the timing of T_1AM administration. Noteworthy, evidence was reported suggesting that some neurological effects elicited after T_1AM administration may be actually produced by its metabolite TA_1 (28, 29). In the present experimental model, TA_1 administration was ineffective in restoring LTP. However, it is known that T_1AM can cross the plasma membrane, and deamination to TA_1 may occur intracellularly (60). Therefore, we cannot exclude that some intracellular effects of T_1AM-derived TA_1 may not be reproduced by the administration of exogenous TA_1.

Also, we aimed at evaluating whether T_3, the putative precursor of T_1AM, could reproduce T_1AM effects. Although T_1AM is supposed to derive from T_3, the use of the latter was ineffective in

preventing Aβ-induced inhibition of LTP and this may be due to the low rate of local T_3 to T_1AM conversion.

Our *in vitro* results encouraged us to investigate the effects of T_1AM treatment *in vivo.* In a previous investigation, we showed that in mhAPP mice, early EC synaptic dysfunction is associated with behavioral deficits in associative memory tasks that require intact EC function (35, 36). T_1AM i.c.v. administration was performed at a dosage previously shown to induce behavioral effects and to increase tissue T_1AM levels by about one order of magnitude over the baseline (27, 61). The treatment was able to ameliorate associative memory in mhAPP mice at an early stage of neurodegeneration, as assessed through the OPRT and OPCRT tests. This finding is consistent with the results of the electrophysiological studies, further supports the protective role of T_1AM in AD models, and may potentially open new therapeutic perspectives based on the T_1AM-TAAR1 pathway. Interestingly, there is evidence that the cognitive impairment produced by scopolamine can also be rescued by T_1AM (27, 62).

We limited our study to the identification of the main cell surface target mediating the neuronal effects of T_1AM in Aβ-induced neuronal impairment and did not evaluate the intracellular pathways responsible for T_1AM effects. However, activation of stress-related protein kinases, such as JNK and p38 MAPK, appears to be a key event in Aβ-dependent neuronal impairment. In particular, these kinases are strongly activated in EC slices exposed to high levels of Aβ (33, 34, 63) and their level of phosphorylation is increased in the EC of mhAPP mice (35). It is noteworthy that both JNK and p38 MAPK inhibition prevented Aβ-induced synaptic plasticity impairment in hippocampal (64) and EC slices (33, 34), and ameliorated behavioural deficits in mhAPP mice (35, 65). Conversely, T_1AM-$TAAR_1$ axis can activate intracellular pathways ultimately leading to the increase in ERK1/2 phosphorylation and c-fos expression (27, 66, 67) that have been demonstrated to play a fundamental role in LTP mechanisms and in memory processes (68, 69).

Therefore, T_1AM neuroprotection may be achieved through the modulation of intracellular pathways counteracting cell stress signaling. In any case, the quick T_1AM metabolism shown in Figure 4 suggests that T_1AM acts by triggering a cascade of events whose final effects persist even after its concentration is normalized.

It must be acknowledged that our investigation has several limitations and further experimental work will be necessary to unravel its implications on the elusive links existing between TH signaling, Aβ toxicity, and AD. First of all, Aβ accumulation is a pathological hallmark of AD, but its causal role on the development and progression of this disease is still controversial (70, 71), and mhAPP mouse cannot be regarded as a standard model of AD. In addition, while LTP is one of the major basic mechanisms of memory and it is affected at an early stage in models of Aβ toxicity, the link between LTP impairment and cognitive dysfunction is obscure, since the latter is likely to represent the final outcome of a complex and still largely unknown pathophysiological process.

On the other hand, the role of T_1AM in the context of TH-induced neuroprotection requires further investigation. Alterations in thyroid function have been linked to the pathogenesis of AD and other dementias. Evidence coming from preclinical studies suggests that TH may modulate APP gene splicing and protein processing, inducing a reduction in the synthesis of Aβ(1-42) oligomers (14), which represent the main soluble species that induce neuronal impairment in the early stages of AD (72). With regard to clinical studies, the assay of TH levels in serum and cerebrospinal fluid showed that both subclinical hypothyroidism and hyperthyroidism represent risk factors for AD (73-76). T_1AM allegedly derives from T3 (46), and now we report that some protective properties of T_1AM are not reproduced by T3. However, at present there is no evidence that local or systemic TH administration may increase brain T_1AM level, nor that the putative beneficial effects of T3 are reproduced by T_1AM.

In conclusion, our study supports the concept that T_1AM and $TAAR_1$ are part of an endogenous system that can be modulated to prevent synaptic and behavioral deficits associated with Aβ-toxicity. Since T_1AM and synthetic analogues appear to elicit pro-learning effects also after systemic administration (67), our results encourage further investigations aimed at determining whether the development of $TAAR_1$ agonists may represent a novel strategy for the treatment of Aβ-related neurodegenerative disorders (77).

Acknowledgements

We gratefully acknowledge R. Di Renzo for technical assistance, Dr. F. Biondi for the excellent animal care, Dr F. Tozzi for helping with the graphical elaboration, and Dr. S. Espinoza for providing TAAR1 knockout mice. This work was supported by the CNR Research Project Nanomax-Nanobrain and by a grant from Pisa University (PRA 2018 to RZ).

Author Disclosure Statement

No competing financial interests exist for any author.

Corresponding author:

Dr. Nicola Origlia
CNR Neuroscience Institute
Via Moruzzi 1
56124 Pisa
Italy

References

1. Bernal J 2000 Thyroid Hormones in Brain Development and Function. In: De Groot LJ, Beck-Peccoz P, Chrousos G, Dungan K, Grossman A, Hershman JM, Koch C, McLachlan R, New M, Rebar R, Singer F, Vinik A, Weickert MO, (eds) Endotext. Vol., South Dartmouth (MA).
2. Volpato S, Guralnik JM, Fried LP, Remaley AT, Cappola AR, Launer LJ 2002 Serum thyroxine level and cognitive decline in euthyroid older women. Neurology **58**:1055-1061.
3. Sampaolo S, Campos-Barros A, Mazziotti G, Carlomagno S, Sannino V, Amato G, Carella C, Di Iorio G 2005 Increased cerebrospinal fluid levels of 3,3',5'-triiodothyronine in patients with Alzheimer's disease. The Journal of clinical endocrinology and metabolism **90**:198-202.
4. Johansson P, Almqvist EG, Johansson JO, Mattsson N, Hansson O, Wallin A, Blennow K, Zetterberg H, Svensson J 2013 Reduced cerebrospinal fluid level of thyroxine in patients with Alzheimer's disease. Psychoneuroendocrinology **38**:1058-1066.
5. Accorroni A, Giorgi FS, Donzelli R, Lorenzini L, Prontera C, Saba A, Vergallo A, Tognoni G, Siciliano G, Baldacci F, Bonuccelli U, Clerico A, Zucchi R 2017 Thyroid hormone levels in the cerebrospinal fluid correlate with disease severity in euthyroid patients with Alzheimer's disease. Endocrine **55**:981-984.
6. Luo L, Yano N, Mao Q, Jackson IM, Stopa EG 2002 Thyrotropin releasing hormone (TRH) in the hippocampus of Alzheimer patients. Journal of Alzheimer's disease : JAD **4**:97-103.
7. Davis JD, Podolanczuk A, Donahue JE, Stopa E, Hennessey JV, Luo LG, Lim YP, Stern RA 2008 Thyroid hormone levels in the prefrontal cortex of post-mortem brains of Alzheimer's disease patients. Curr Aging Sci **1**:175-181.
8. Rami A, Krieglstein J 1992 Thyroxine attenuates hippocampal neuronal damage caused by ischemia in the rat. Life sciences **50**:645-650.
9. Losi G, Garzon G, Puia G 2008 Nongenomic regulation of glutamatergic neurotransmission in hippocampus by thyroid hormones. Neuroscience **151**:155-163.
10. Desouza LA, Ladiwala U, Daniel SM, Agashe S, Vaidya RA, Vaidya VA 2005 Thyroid hormone regulates hippocampal neurogenesis in the adult rat brain. Molecular and cellular neurosciences **29**:414-426.
11. Alzoubi KH, Gerges NZ, Alkadhi KA 2005 Levothyroxin restores hypothyroidism-induced impairment of LTP of hippocampal CA1: electrophysiological and molecular studies. Exp Neurol **195**:330-341.
12. Alzoubi KH, Gerges NZ, Aleisa AM, Alkadhi KA 2009 Levothyroxin restores hypothyroidism-induced impairment of hippocampus-dependent learning and memory: Behavioral, electrophysiological, and molecular studies. Hippocampus **19**:66-78.
13. Belakavadi M, Dell J, Grover GJ, Fondell JD 2011 Thyroid hormone suppression of beta-amyloid precursor protein gene expression in the brain involves multiple epigenetic regulatory events. Molecular and cellular endocrinology **339**:72-80.
14. Latasa MJ, Belandia B, Pascual A 1998 Thyroid hormones regulate beta-amyloid gene splicing and protein secretion in neuroblastoma cells. Endocrinology **139**:2692-2698.
15. Belandia B, Latasa MJ, Villa A, Pascual A 1998 Thyroid hormone negatively regulates the transcriptional activity of the beta-amyloid precursor protein gene. The Journal of biological chemistry **273**:30366-30371.
16. Shabani S, Sarkaki A, Ali Mard S, Ahangarpour A, Khorsandi L, Farbood Y 2016 Central and peripheral administrations of levothyroxine improved memory performance and amplified brain electrical activity in the rat model of Alzheimer's disease. Neuropeptides **59**:111-116.
17. Fu AL, Zhou CY, Chen X 2010 Thyroid hormone prevents cognitive deficit in a mouse model of Alzheimer's disease. Neuropharmacology **58**:722-729.
18. Farbood Y, Shabani S, Sarkaki A, Mard SA, Ahangarpour A, Khorsandi L 2017 Peripheral and central administration of T3 improved the histological changes, memory and the dentate gyrus electrophysiological activity in an animal model of Alzheimer's disease. Metab Brain Dis **32**:693-701.

19. Shabani S, Farbood Y, Mard SA, Sarkaki A, Ahangarpour A, Khorsandi L 2018 The regulation of pituitary-thyroid abnormalities by peripheral administration of levothyroxine increased brain-derived neurotrophic factor and reelin protein expression in an animal model of Alzheimer's disease. Canadian journal of physiology and pharmacology **96**:275-280.

20. Flamant F, Cheng SY, Hollenberg AN, Moeller LC, Samarut J, Wondisford FE, Yen PM, Refetoff S 2017 Thyroid Hormone Signaling Pathways: Time for a More Precise Nomenclature. Endocrinology **158**:2052-2057.

21. Scanlan TS, Suchland KL, Hart ME, Chiellini G, Huang Y, Kruzich PJ, Frascarelli S, Crossley DA, Bunzow JR, Ronca-Testoni S, Lin ET, Hatton D, Zucchi R, Grandy DK 2004 3-Iodothyronamine is an endogenous and rapid-acting derivative of thyroid hormone. Nature medicine **10**:638-642.

22. Zucchi R, Chiellini G, Scanlan TS, Grandy DK 2006 Trace amine-associated receptors and their ligands. British journal of pharmacology **149**:967-978.

23. Rutigliano G, Accorroni A, Zucchi R 2017 The Case for TAAR1 as a Modulator of Central Nervous System Function. Front Pharmacol **8**:987.

24. Revel FG, Moreau JL, Gainetdinov RR, Ferragud A, Velazquez-Sanchez C, Sotnikova TD, Morairty SR, Harmeier A, Groebke Zbinden K, Norcross RD, Bradaia A, Kilduff TS, Biemans B, Pouzet B, Caron MG, Canales JJ, Wallace TL, Wettstein JG, Hoener MC 2012 Trace amine-associated receptor 1 partial agonism reveals novel paradigm for neuropsychiatric therapeutics. Biological psychiatry **72**:934-942.

25. Revel FG, Moreau JL, Gainetdinov RR, Bradaia A, Sotnikova TD, Mory R, Durkin S, Zbinden KG, Norcross R, Meyer CA, Metzler V, Chaboz S, Ozmen L, Trube G, Pouzet B, Bettler B, Caron MG, Wettstein JG, Hoener MC 2011 TAAR1 activation modulates monoaminergic neurotransmission, preventing hyperdopaminergic and hypoglutamatergic activity. Proceedings of the National Academy of Sciences of the United States of America **108**:8485-8490.

26. Revel FG, Moreau JL, Pouzet B, Mory R, Bradaia A, Buchy D, Metzler V, Chaboz S, Groebke Zbinden K, Galley G, Norcross RD, Tuerck D, Bruns A, Morairty SR, Kilduff TS, Wallace TL, Risterucci C, Wettstein JG, Hoener MC 2013 A new perspective for schizophrenia: TAAR1 agonists reveal antipsychotic- and antidepressant-like activity, improve cognition and control body weight. Molecular psychiatry **18**:543-556.

27. Manni ME, De Siena G, Saba A, Marchini M, Landucci E, Gerace E, Zazzeri M, Musilli C, Pellegrini-Giampietro D, Matucci R, Zucchi R, Raimondi L 2013 Pharmacological effects of 3-iodothyronamine (T1AM) in mice include facilitation of memory acquisition and retention and reduction of pain threshold. British journal of pharmacology **168**:354-362.

28. Laurino A, De Siena G, Saba A, Chiellini G, Landucci E, Zucchi R, Raimondi L 2015 In the brain of mice, 3-iodothyronamine (T1AM) is converted into 3-iodothyroacetic acid (TA1) and it is included within the signaling network connecting thyroid hormone metabolites with histamine. European journal of pharmacology **761**:130-134.

29. Musilli C, De Siena G, Manni ME, Logli A, Landucci E, Zucchi R, Saba A, Donzelli R, Passani MB, Provensi G, Raimondi L 2014 Histamine mediates behavioural and metabolic effects of 3-iodothyroacetic acid, an endogenous end product of thyroid hormone metabolism. British journal of pharmacology **171**:3476-3484.

30. Laurino A, Landucci E, Resta F, De Siena G, Matucci R, Masi A, Raimondi L 2018 3-Iodothyroacetic acid (TA1), a by-product of thyroid hormone metabolism, reduces the hypnotic effect of ethanol without interacting at GABA-A receptors. Neurochemistry international **115**:31-36.

31. Braak H, Braak E 1991 Demonstration of amyloid deposits and neurofibrillary changes in whole brain sections. Brain Pathol **1**:213-216.

32. Stranahan AM, Mattson MP 2010 Selective vulnerability of neurons in layer II of the entorhinal cortex during aging and Alzheimer's disease. Neural Plast **2010**:108190.

33. Origlia N, Righi M, Capsoni S, Cattaneo A, Fang F, Stern DM, Chen JX, Schmidt AM, Arancio O, Yan SD, Domenici L 2008 Receptor for advanced glycation end product-dependent activation of p38 mitogen-activated protein kinase contributes to amyloid-beta-mediated cortical synaptic dysfunction. The Journal of neuroscience **28**:3521-3530.

34. Origlia N, Bonadonna C, Rosellini A, Leznik E, Arancio O, Yan SS, Domenici L 2010 Microglial receptor for advanced glycation end product-dependent signal pathway drives beta-amyloid-induced synaptic depression and long-term depression impairment in entorhinal cortex. The Journal of neuroscience **30**:11414-11425.

35. Criscuolo C, Fontebasso V, Middei S, Stazi M, Ammassari-Teule M, Yan SS, Origlia N 2017 Entorhinal Cortex dysfunction can be rescued by inhibition of microglial RAGE in an Alzheimer's disease mouse model. Scientific reports **7**:42370.

36. Wilson DI, Langston RF, Schlesiger MI, Wagner M, Watanabe S, Ainge JA 2013 Lateral entorhinal cortex is critical for novel object-context recognition. Hippocampus **23**:352-366.

37. Wilson DI, Watanabe S, Milner H, Ainge JA 2013 Lateral entorhinal cortex is necessary for associative but not nonassociative recognition memory. Hippocampus **23**:1280-1290.

38. Origlia N, Criscuolo C, Arancio O, Yan SS, Domenici L 2014 RAGE inhibition in microglia prevents ischemia-dependent synaptic dysfunction in an amyloid-enriched environment. The Journal of neuroscience **34**:8749-8760.

39. Hart ME, Suchland KL, Miyakawa M, Bunzow JR, Grandy DK, Scanlan TS 2006 Trace amine-associated receptor agonists: synthesis and evaluation of thyronamines and related analogues. Journal of medicinal chemistry **49**:1101-1112.

40. Yan Y, Liu Y, Sorci M, Belfort G, Lustbader JW, Yan SS, Wang C 2007 Surface plasmon resonance and nuclear magnetic resonance studies of ABAD-Abeta interaction. Biochemistry **46**:1724-1731.

41. Origlia N, Arancio O, Domenici L, Yan SS 2009 MAPK, beta-amyloid and synaptic dysfunction: the role of RAGE. Expert Rev Neurother **9**:1635-1645.

42. Haley TJ, McCormick WG 1957 Pharmacological effects produced by intracerebral injection of drugs in the conscious mouse. Br J Pharmacol Chemother **12**:12-15.

43. Patel TP, Gullotti DM, Hernandez P, O'Brien WT, Capehart BP, Morrison B, 3rd, Bass C, Eberwine JE, Abel T, Meaney DF 2014 An open-source toolbox for automated phenotyping of mice in behavioral tasks. Front Behav Neurosci **8**:349.

44. Saba A, Chiellini G, Frascarelli S, Marchini M, Ghelardoni S, Raffaelli A, Tonacchera M, Vitti P, Scanlan TS, Zucchi R 2010 Tissue distribution and cardiac metabolism of 3-iodothyronamine. Endocrinology **151**:5063-5073.

45. Assadi-Porter FM, Reiland H, Sabatini M, Lorenzini L, Carnicelli V, Rogowski M, Selen Alpergin ES, Tonelli M, Ghelardoni S, Saba A, Zucchi R, Chiellini G 2018 Metabolic Reprogramming by 3-Iodothyronamine (T1AM): A New Perspective to Reverse Obesity through Co-Regulation of Sirtuin 4 and 6 Expression. Int J Mol Sci **19:**E1535.

46. Hoefig CS, Zucchi R, J. K 2016 Thyronamines and derivatives: Physiological relevance, pharmacological actions and future research directions. Thyroid **26:**1656-1673.

47. Laurino A, Landucci E, Resta F, De Siena G, Pellegrini-Giampietro DE, Masi A, Mannaioni G, Raimondi L 2018 Anticonvulsant and Neuroprotective Effects of the Thyroid Hormone Metabolite 3-Iodothyroacetic Acid. Thyroid **28**:1387-1397.

48. Kohrle J, Biebermann H 2019 3-iodothyronamine - a thyroid hormone metabolite with distinct target profiles and mode of action. Endocr Rev **40:**602-630.

49. Mucke L, Masliah E, Yu GQ, Mallory M, Rockenstein EM, Tatsuno G, Hu K, Kholodenko D, Johnson-Wood K, McConlogue L 2000 High-level neuronal expression of abeta 1-42 in wild-type human amyloid protein precursor transgenic mice: synaptotoxicity without plaque formation. The Journal of neuroscience **20**:4050-4058.

50. Zucchi R, Accorroni A, Chiellini G 2014 Update on 3-iodothyronamine and its neurological and metabolic actions. Frontiers in physiology **5**:402.

51. Gomez-Isla T, Price JL, McKeel DW, Jr., Morris JC, Growdon JH, Hyman BT 1996 Profound loss of layer II entorhinal cortex neurons occurs in very mild Alzheimer's disease. The Journal of neuroscience **16**:4491-4500.

52. Scheff SW, Price DA, Schmitt FA, Mufson EJ 2006 Hippocampal synaptic loss in early Alzheimer's disease and mild cognitive impairment. Neurobiol Aging **27**:1372-1384.

53. Dinter J, Muhlhaus J, Jacobi SF, Wienchol CL, Coster M, Meister J, Hoefig CS, Muller A, Kohrle J, Gruters A, Krude H, Mittag J, Schoneberg T, Kleinau G, Biebermann H 2015 3-iodothyronamine differentially modulates alpha-2A-adrenergic receptor-mediated signaling. Journal of molecular endocrinology **54**:205-216.

54. Kleinau G, Pratzka J, Nurnberg D, Gruters A, Fuhrer-Sakel D, Krude H, Kohrle J, Schoneberg T, Biebermann H 2011 Differential modulation of Beta-adrenergic receptor signaling by trace amine-associated receptor 1 agonists. PloS one **6**:e27073.

55. Snead AN, Santos MS, Seal RP, Miyakawa M, Edwards RH, Scanlan TS 2007 Thyronamines inhibit plasma membrane and vesicular monoamine transport. ACS chemical biology **2**:390-398.

56. Espinoza S, Lignani G, Caffino L, Maggi S, Sukhanov I, Leo D, Mus L, Emanuele M, Ronzitti G, Harmeier A, Medrihan L, Sotnikova TD, Chieregatti E, Hoener MC, Benfenati F, Tucci V, Fumagalli F, Gainetdinov RR 2015 TAAR1 Modulates Cortical Glutamate NMDA Receptor Function. Neuropsychopharmacology **40**:2217-2227.

57. Coster M, Biebermann H, Schoneberg T, Staubert C 2015 Evolutionary Conservation of 3-Iodothyronamine as an Agonist at the Trace Amine-Associated Receptor 1. European thyroid journal **4**:9-20.

58. Lorenzini L, Ghelardoni S, Saba A, Sacripanti G, Chiellini G, Zucchi R 2017 Recovery of 3-Iodothyronamine and Derivatives in Biological Matrixes: Problems and Pitfalls. Thyroid **27**:1323-1331.

59. Puzzo D, Privitera L, Leznik E, Fa M, Staniszewski A, Palmeri A, Arancio O 2008 Picomolar amyloid-beta positively modulates synaptic plasticity and memory in hippocampus. The Journal of neuroscience **28**:14537-14545.

60. Lehmphul I, Hoefig CS, Kohrle J 2018 3-Iodothyronamine reduces insulin secretion in vitro via a mitochondrial mechanism. Molecular and cellular endocrinology **460**:219-228.

61. Laurino A, De Siena G, Resta F, Masi A, Musilli C, Zucchi R, Raimondi L 2015 3-iodothyroacetic acid, a metabolite of thyroid hormone, induces itch and reduces threshold to noxious and to painful heat stimuli in mice. British journal of pharmacology **172**:1859-1868.

62. Laurino A, Lucenteforte E, De Siena G, Raimondi L 2017 The impact of scopolamine pretreatment on 3-iodothyronamine (T1AM) effects on memory and pain in mice. Hormones and behavior **94**:93-96.

63. Takuma K, Yao J, Huang J, Xu H, Chen X, Luddy J, Trillat AC, Stern DM, Arancio O, Yan SS 2005 ABAD enhances Abeta-induced cell stress via mitochondrial dysfunction. FASEB journal **19**:597-598.

64. Wang Q, Walsh DM, Rowan MJ, Selkoe DJ, Anwyl R 2004 Block of long-term potentiation by naturally secreted and synthetic amyloid beta-peptide in hippocampal slices is mediated via activation of the kinases c-Jun N-terminal kinase, cyclin-dependent kinase 5, and p38 mitogen-activated protein kinase as well as metabotropic glutamate receptor type 5. The Journal of neuroscience **24**:3370-3378.

65. Rutigliano G, Stazi M, Arancio O, Watterson DM, Origlia N 2018 An isoform-selective p38alpha mitogen-activated protein kinase inhibitor rescues early entorhinal cortex dysfunctions in a mouse model of Alzheimer's disease. Neurobiol Aging **70**:86-91.

66. Harmeier A, Obermueller S, Meyer CA, Revel FG, Buchy D, Chaboz S, Dernick G, Wettstein JG, Iglesias A, Rolink A, Bettler B, Hoener MC 2015 Trace amine-associated receptor 1 activation silences GSK3beta signaling of TAAR1 and D2R heteromers. European neuropsychopharmacology **25**:2049-2061.

67. Bellusci L, Laurino A, Sabatini M, Sestito S, Lenzi P, Raimondi L, Rapposelli S, Biagioni F, Fornai F, Salvetti A, Rossi L, Zucchi R, Chiellini G 2017 New Insights into the Potential Roles of 3-Iodothyronamine (T1AM) and Newly Developed Thyronamine-Like TAAR1 Agonists in Neuroprotection. Front Pharmacol **8**:905.

68. Giese KP, Mizuno K 2013 The roles of protein kinases in learning and memory. Learn Mem **20**:540-552.

69. Minatohara K, Akiyoshi M, Okuno H 2015 Role of Immediate-Early Genes in Synaptic Plasticity and Neuronal Ensembles Underlying the Memory Trace. Front Mol Neurosci **8**:78.

70. Doig AJ, Del Castillo-Frias MP, Berthoumieu O, Tarus B, Nasica-Labouze J, Sterpone F, Nguyen PH, Hooper NM, Faller P, Derreumaux P 2017 Why Is Research on Amyloid-beta Failing to Give New Drugs for Alzheimer's Disease? ACS chemical neuroscience **8**:1435-1437.

71. Ricciarelli R, Fedele E 2017 The Amyloid Cascade Hypothesis in Alzheimer's Disease: It's Time to Change Our Mind. Current neuropharmacology **15**:926-935.

72. Palop JJ, Mucke L 2010 Amyloid-beta-induced neuronal dysfunction in Alzheimer's disease: from synapses toward neural networks. Nature neuroscience **13**:812-818.

73. Ceresini G, Lauretani F, Maggio M, Ceda GP, Morganti S, Usberti E, Chezzi C, Valcavi R, Bandinelli S, Guralnik JM, Cappola AR, Valenti G, Ferrucci L 2009 Thyroid function abnormalities and cognitive impairment in elderly people: results of the Invecchiare in Chianti study. J Am Geriatr Soc **57**:89-93.

74. Hogervorst E, Huppert F, Matthews FE, Brayne C 2008 Thyroid function and cognitive decline in the MRC Cognitive Function and Ageing Study. Psychoneuroendocrinology **33**:1013-1022.

75. Tan ZS, Beiser A, Vasan RS, Au R, Auerbach S, Kiel DP, Wolf PA, Seshadri S 2008 Thyroid function and the risk of Alzheimer disease: the Framingham Study. Archives of internal medicine **168**:1514-1520.

76. Juarez-Cedillo T, Basurto-Acevedo L, Vega-Garcia S, Sanchez-Rodriguez Martha A, Retana-Ugalde R, Juarez-Cedillo E, Gonzalez-Melendez Roberto C, Escobedo-de-la-Pena J 2017 Prevalence of thyroid dysfunction and its impact on cognition in older mexican adults: (SADEM study). J Endocrinol Invest **40**:945-952.

77. Schwartz MD, Canales JJ, Zucchi R, Espinoza S, Sukhanov I, Gainetdinov RR 2018 Trace amine-associated receptor 1: a multimodal therapeutic target for neuropsychiatric diseases. Expert Opin Ther Targets **22**:513-526.

Figure Legends

Figure 1. $TAAR_1$ expression in EC. **A,** Representative Western blot of EC slices homogenates, from control mhAPP mice (1-2) and age-matched WT (3-4) using a polyclonal antibody against $TAAR_1$ and β-tubulin; the $TAAR_1$ protein migrates as 39 kDa. Antibody specificity was confirmed using as a negative control mouse liver samples, where TAAR1 expression has not been reported and quantitative PCR did not provide evidence of significant *taar1* expression. **B**, The plot represents mean±SEM values of $TAAR_1$ band intensity relative to β-tubulin content (n=6 per group). **C,** Immuno-localization of $TAAR_1$ (left column) and neuronal marker NeuN (middle column) in the EC of mhAPP and wild-type mice. Representative images (20×) show that the pattern of $TAAR_1$ fluorescent signal in EC superficial layers of 2-month old mhAPP mice is comparable to that of age-matched wild-type. $TAAR_1$ immunofluorescence co-localizes with the neuronal marker NeuN (merge in the right column); inserts show higher magnification (40x) of cells indicated by arrows. Scale bar=50 µm. **D**, The plot represents mean±SEM values of $TAAR_1$ fluoresent signal, performed as described in the methods section.

Figure 2. Endogenous T_1AM in EC. **A,** HPLC-MS/MS tracings from a representative experiment. The transitions monitored by the mass spectrometry equipment (356.2 → 195.2, 356.2 → 212.2, 356.2 → 339.1) are shown by the blue, red, and green lines, respectively. The tracings were obtained from WT EC, and the lower one includes the internal standard, i.e. deuterated T_1AM (in this case transitions were recalculated as 360.2 → 199.2, 360.2 → 216.2, 360.2 → 343.1). Endogenous T_1AM was identified based on retention time and ratios between transitions. See methods for further details. **B,** Average levels (mean±SEM; n=4 per group) of endogenous T_1AM in mhAPP and non –transgenic WT mice, measured by HPLC-MS/MS in tissue extract of EC slices .

Figure 3. T_1AM rescues the inhibitory effect of Aβ on LTP in entorhinal cortex slices. **A**, Input–output curves. The amplitude is shown as percentage of the maximum amplitude (% of max. ampl.) and plotted as a function of stimulus intensity (Stim. Int.). No significant difference occurred between vehicle-treated, T_1AM (5 μM) and T_3 (5 μM) perfused slices. Inserts show representative FPs recorded at each stimulus intensity, and scale bars correspond to 0.5 mV and 0.5 ms. **B,** LTP expression, induced by HFS, applied after 15 min of baseline recording. The LTP magnitude is expressed as relative amplitude (Rel. Ampl. vs baseline) and it was comparable between vehicle, T_1AM and T_3 treated slices. Data points represent mean±SEM of 8-9 slices per group, derived from at least 4 mice. Inserts show representative FPs recorded during baseline (grey) or after HFS stimulation (black); scale bars correspond to 0.5 mV and 0.5 ms. **C,** LTP expression, shown as in panel B, was blocked by bath application of Aβ (1-42) (200 nM) for 10 min (grey-dotted line). However, LTP was unaffected when Aβ was co-perfused with T_1AM (10 min grey-dotted line). In contrast, T_3 administration for 10 min did not prevent Aβ-induced LTP inhibition. Data points represent mean±SEM of 6-12 slices per group, derived from at least 3 mice. See text for numerical results and statistical significance.

Figure 4. TA_1 administration does not rescue LTP in Aβ-treated slices. **A**, T_1AM and TA_1 average levels in the eluate at different time points after the exogenous administration of 5 μM T_1AM, measured by HPLC-MS/MS. The eluate was divided into fractions collected over 10-15 min intervals, which were sampled for T_1AM and TA_1. The values (mean±SEM of 3 different experiments) are plotted at time points corresponding to the median of each interval. **B**, No effect on LTP expression was observed during administration of exogenous TA_1 (5 μM); co-perfusion of TA_1 with 200 nM Aβ (1-42) was not sufficient to prevent LTP inhibition (grey circles). Data points

represent mean±SEM of 6 slices per group, derived from at least 3 mice. Inserts shows representative FPs recorded during baseline (grey) or after HFS stimulation (black); scale bars correspond to 0.5 mV and 0.5 ms. See text for numerical results and statistical significance.

Figure 5. $TAAR_1$ mediates the protective effect of T_1AM against Aβ-induced inhibition of LTP in EC slices. **A**, Specific $TAAR_1$ antagonist (EPPTB, 5 nM) and agonist (RO5166017, 250 nM) were used in the perfusion of WT control slices (10 min, corresponding to the dark bar). LTP expression was not affected neither by the inhibition (EPPTB) nor by the activation (RO5166017) of $TAAR_1$; **B,** In presence of EPPTB, T_1AM (5 μM) rescue of LTP in Aβ treated slices was completely suppressed (black circles) with respect to slices perfused only with Aβ and T_1AM (grey circles), while EPPTB alone did not modify the response to Aβ (grey diamonds); **C,** A complete rescue of LTP in Aβ-treated EC slices was achieved by co-perfusion with the $TAAR_1$ agonist (RO5166017, grey circles) with significant difference when compared to slices perfused with Aβ alone (white circles); the response to RO5166017 was prevented by EPPTB co-perfusion (black circles).
Data points represent mean±SEM of 5-8 slices per group, derived from at least 3 mice. Inserts shows representative FPs recorded during baseline (grey) or after HFS stimulation (black); scale bars correspond to 0.5 mV and 0.5 ms. See text for numerical results and statistical significance.

Figure 6. Results of *ex-vivo* electrophysiological experiments performed to assess LTP in EC slices derived from five heterozygous TAAR1 knockout mice (TAAR1 KO, number of EC slices=6), and three wild type littermates (WT, number of EC slices=3). Data represent mean±SEM of the amplitude after high frequency stimulation (HFS) normalized to baseline amplitude and averaged over 40 min after HFS. * = $P<0.05$ vs TAAR1 KO after HFS, by two-way ANOVA and Tukey's test.

Figure 7. T_1AM-mediated activation of $TAAR_1$ rescues LTP impairment in mhAPP EC slices at an early stage of neurodegeneration. **A,** In 2-month old mhAPP mice, HFS of EC superficial layer does not induce a stable LTP (white circles); however, acute perfusion of T_1AM (5 µM) for 10 min, prevented LTP impairment (grey circles). The protective effect induced by T_1AM was abolished in mhAPP slices that were co-perfused with the $TAAR_1$ antagonist EPPTB (5 nM, 10 min; black circles). **B,** EC-LTP was normally expressed in mhAPP slices perfused with the $TAAR_1$ agonist (RO5166017, 250 nM, grey circles) with respect to mhAPP untreated slices (white circles).

Data points represent mean±SEM of 5-7 slices per group, derived from at least 3 mice. Inserts shows representative FPs recorded during baseline (grey) or after HFS stimulation (black); scale bars correspond to 0.5 mV and 0.5 ms. See text for numerical results and statistical significance.

Figure 8. Behavioral analysis. **A,** plot representing the total distance covered in the exploration of the arena during the open field test. **B,** plot representing the average fraction of time spent exploring the center of the arena during the trials in the open field test. **C** and **D**, memory performance, expressed by the discrimination index (DI) of mice in the novel object place recognition task (OPRT) and the novel object place/contest recognition task (OPCRT), which were performed as reported in the schematic drawing. OPRT: during the sample trial mice were allowed to explore two different novel objects for 3 min, while in the test trial they explored two copies of one of the previously presented objects in the same context. OPCRT: in sample trial 1 explored two objects in context 1 (3 min), mice were then exposed to context 2 (3 min) and left to explore the same two objects but in opposite position from where they were in context 1; In the test trial (3 min), two copies of one of the previously presented objects were presented within one of the contexts.

Results are plotted as mean±SEM of 6 mice per group; * = $p < 0.05$ *vs*. all other groups.

Fig. 1

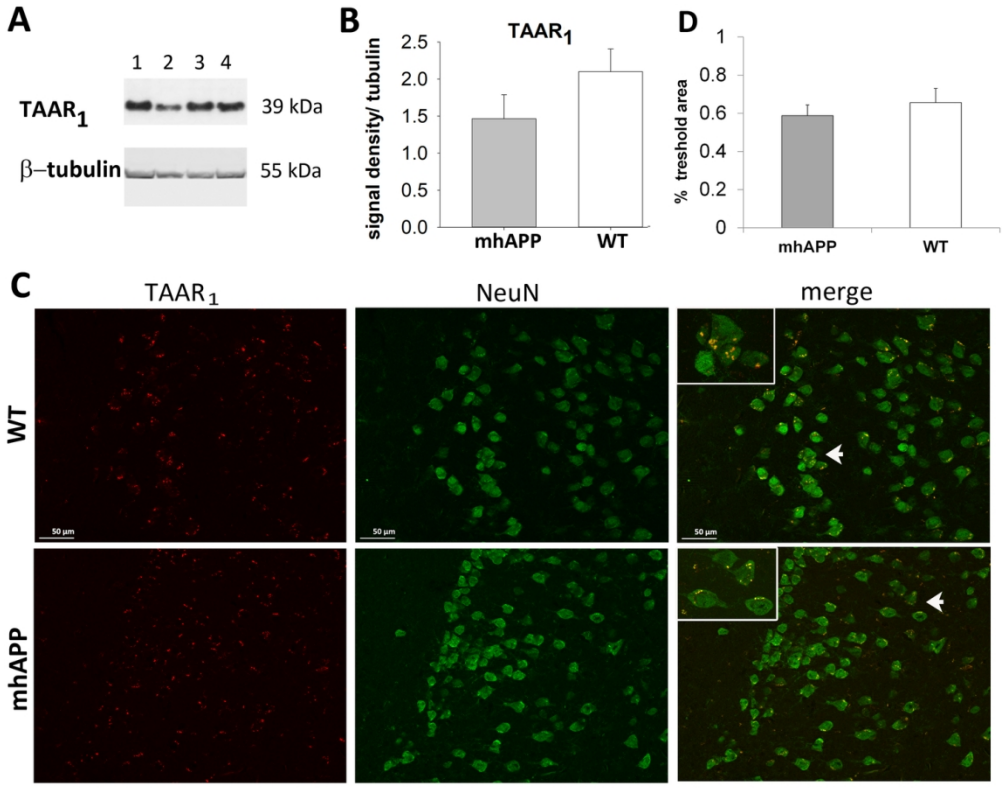
A
1 2 3 4
TAAR1
39 kDa
β–tubulin
55 kDa
B
TAAR1
signal density/ tubulin
2.5
2.0
1.5
1.0
0.5
0.0
mhAPP
WT
D
% treshold area
1
0.8
0.6
0.4
0.2
0
mhAPP
WT
C
TAAR1
NeuN
merge
WT
mhAPP
50 µm

Fig. 2

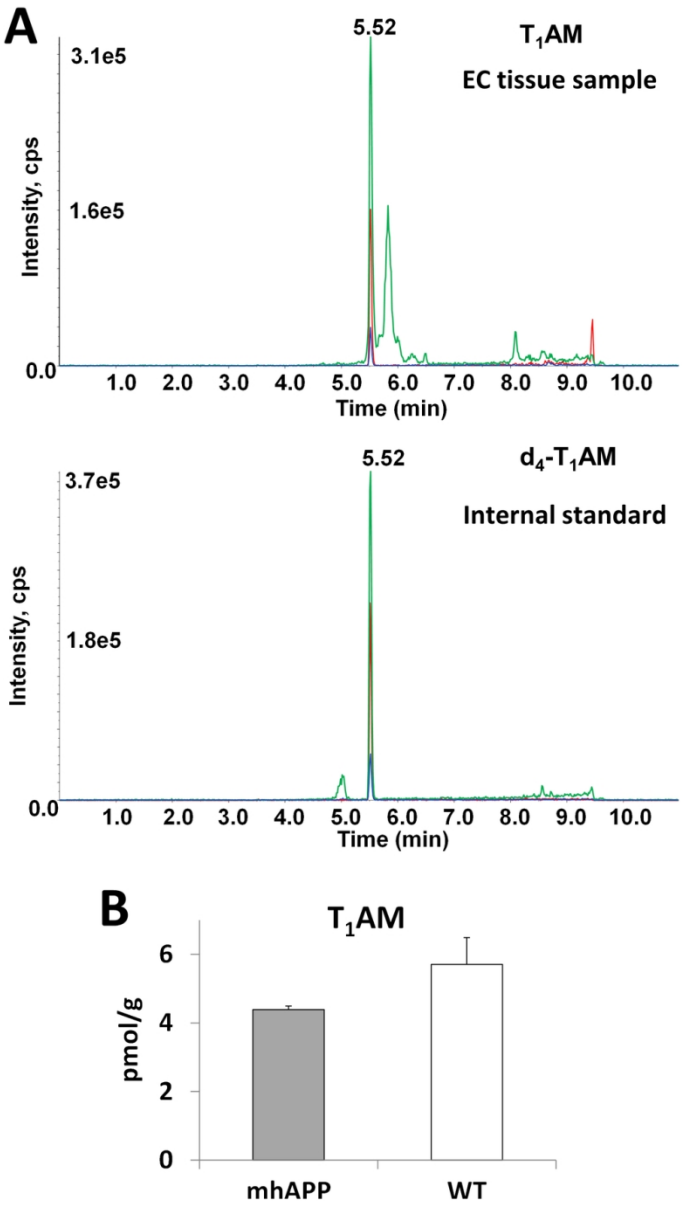
A
5.52
T1AM
EC tissue sample
3.1e5
1.6e5
Intensity, cps
0.0
1.0 2.0 3.0 4.0 5.0 6.0 7.0 8.0 9.0 10.0
Time (min)
5.52
d4-T1AM
Internal standard
3.7e5
1.8e5
Intensity, cps
0.0
1.0 2.0 3.0 4.0 5.0 6.0 7.0 8.0 9.0 10.0
Time (min)
B
T1AM
pmol/g
6
4
2
0
mhAPP
WT

Fig. 3

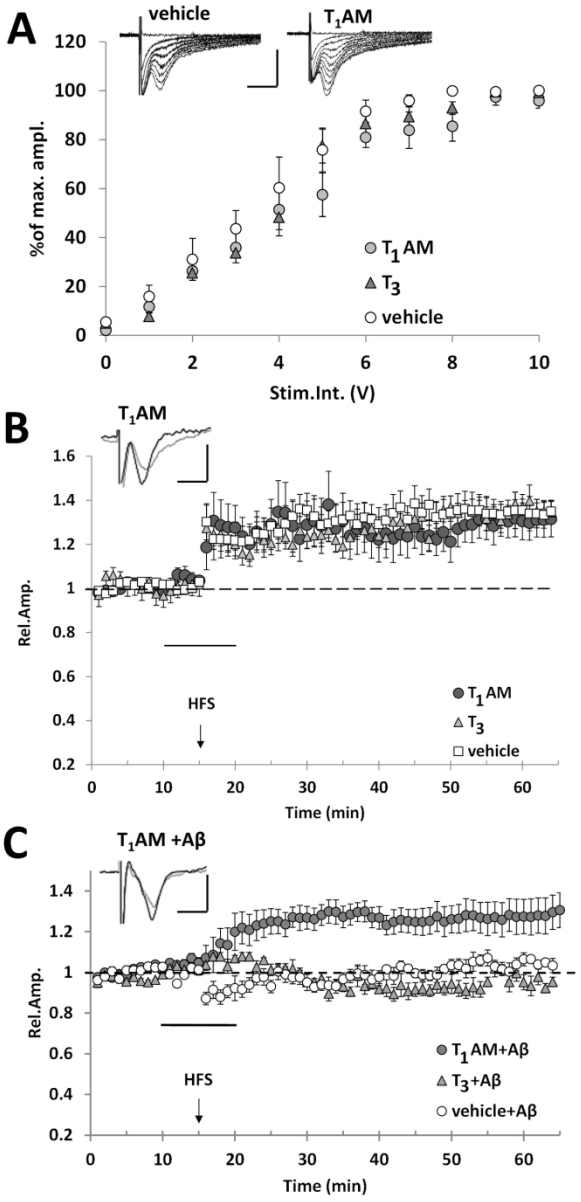
A
vehicle
T1AM
%of max. ampl.
Stim.Int. (V)
T1 AM
T3
vehicle
B
T1AM
Rel.Amp.
HFS
T1 AM
T3
vehicle
Time (min)
C
T1AM +Aβ
Rel.Amp.
HFS
T1 AM+Aβ
T3+Aβ
vehicle+Aβ
Time (min)

Fig. 4

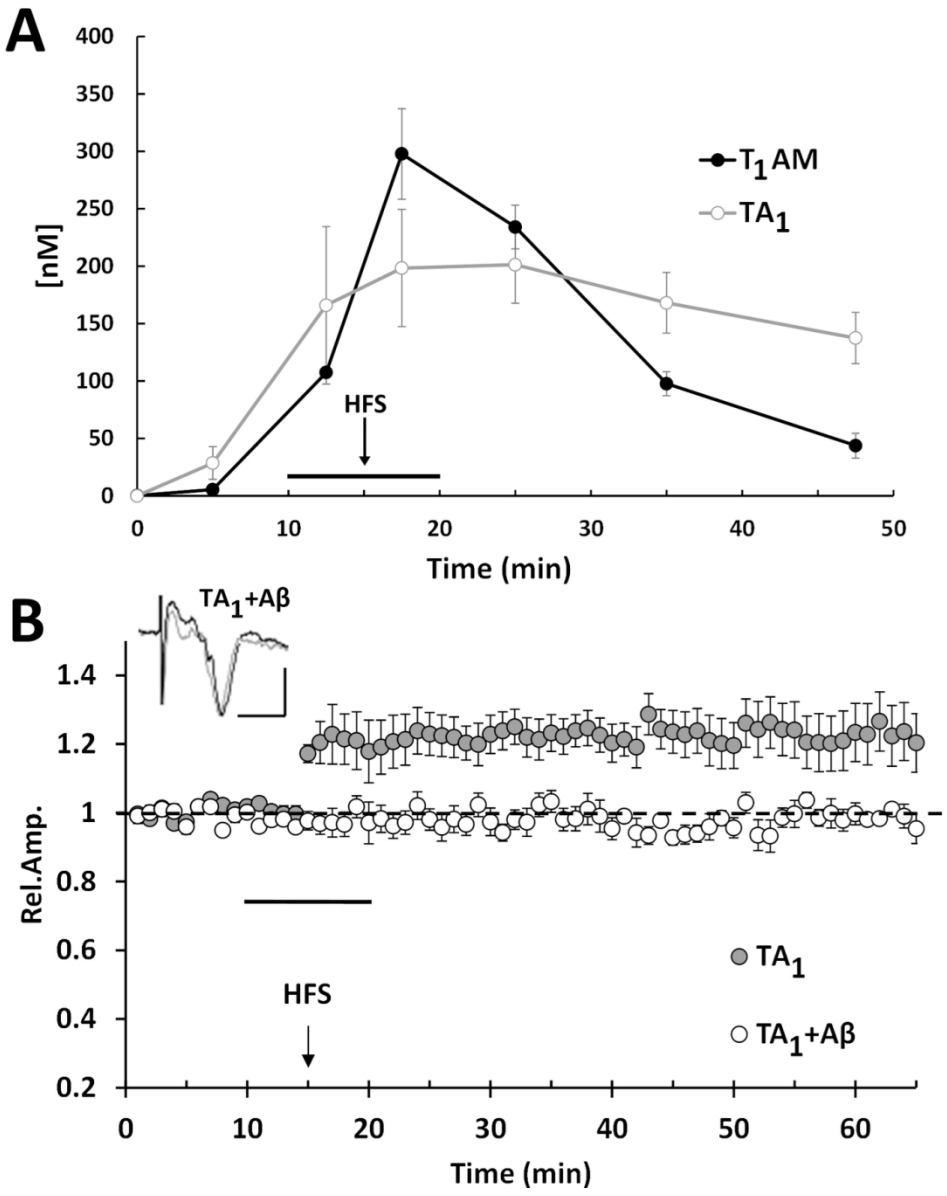
A
400
350
300
250
200
150
100
50
0
[nM]
T1 AM
TA1
HFS
0
10
20
30
40
50
Time (min)
B
TA1+Aβ
1.4
1.2
1
0.8
0.6
0.4
0.2
Rel.Amp.
TA1
TA1+Aβ
HFS
0
10
20
30
40
50
60
Time (min)

Fig. 5

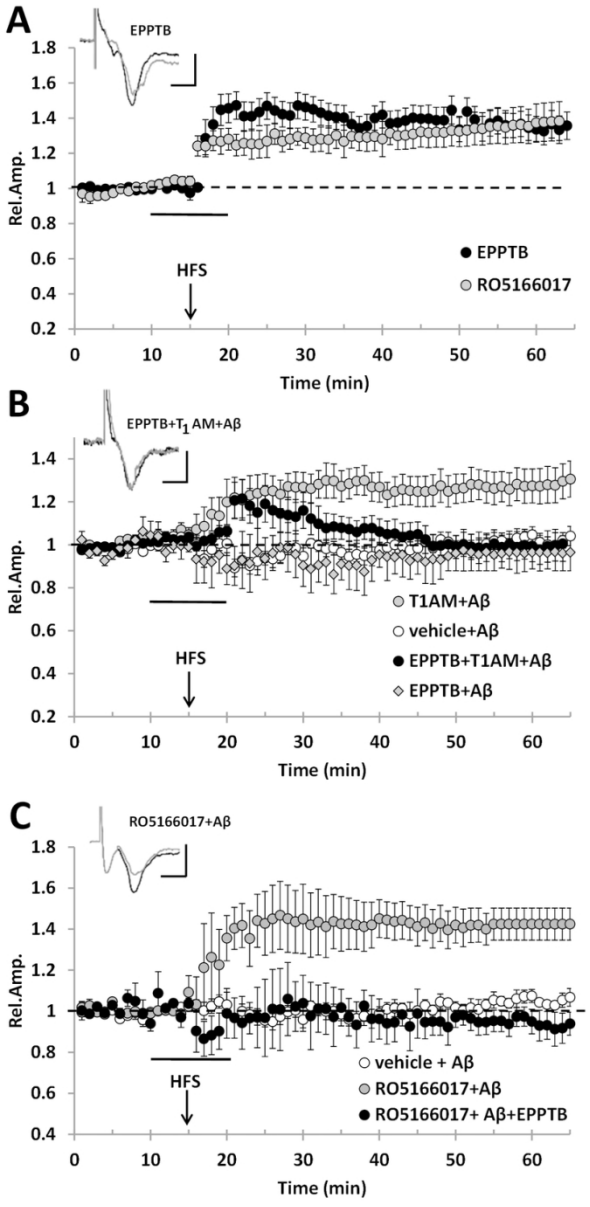
A
EPPTB
Rel.Amp.
HFS
EPPTB
RO5166017
Time (min)
B
EPPTB+T1 AM+Aβ
Rel.Amp.
HFS
T1AM+Aβ
vehicle+Aβ
EPPTB+T1AM+Aβ
EPPTB+Aβ
Time (min)
C
RO5166017+Aβ
Rel.Amp.
HFS
vehicle + Aβ
RO5166017+Aβ
RO5166017+ Aβ+EPPTB
Time (min)

Fig. 6

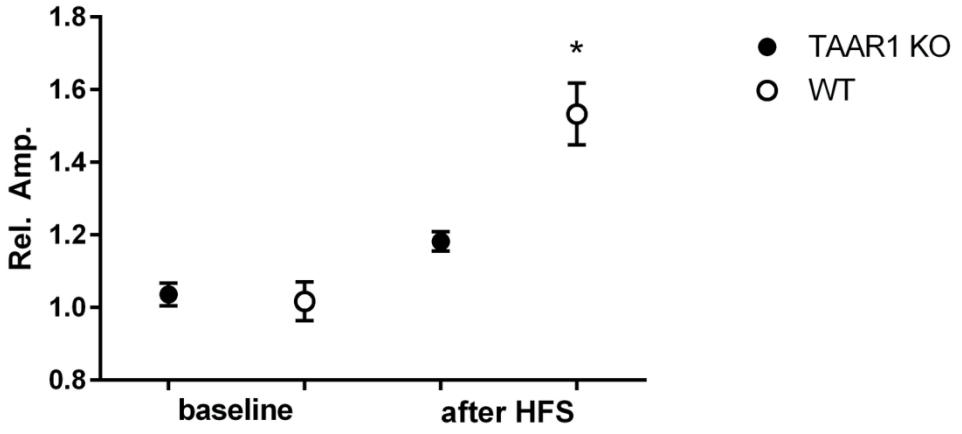

Fig. 7

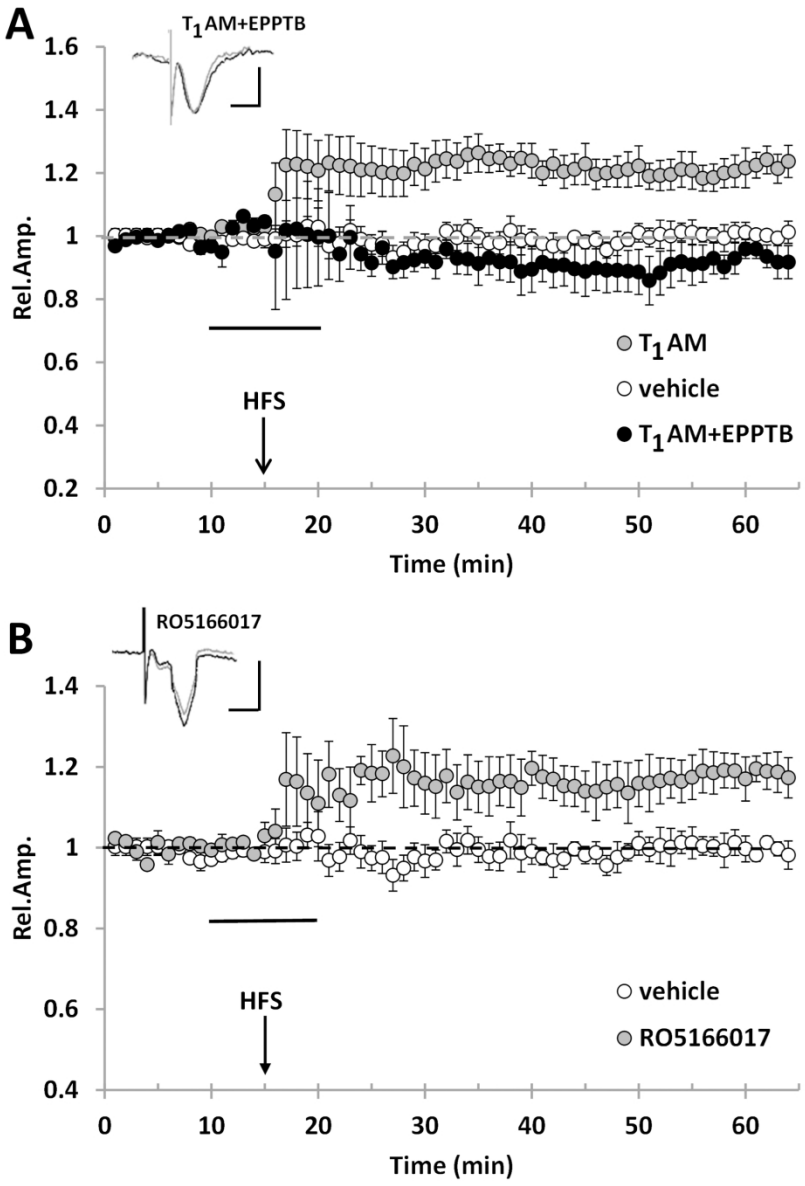
A
T1AM+EPPTB
1.6
1.4
1.2
1
0.8
0.6
0.4
0.2
Rel.Amp.
HFS
T1AM
vehicle
T1AM+EPPTB
0
10
20
30
40
50
60
Time (min)
B
RO5166017
1.4
1.2
1
0.8
0.6
0.4
Rel.Amp.
HFS
vehicle
RO5166017
0
10
20
30
40
50
60
Time (min)

Fig. 8

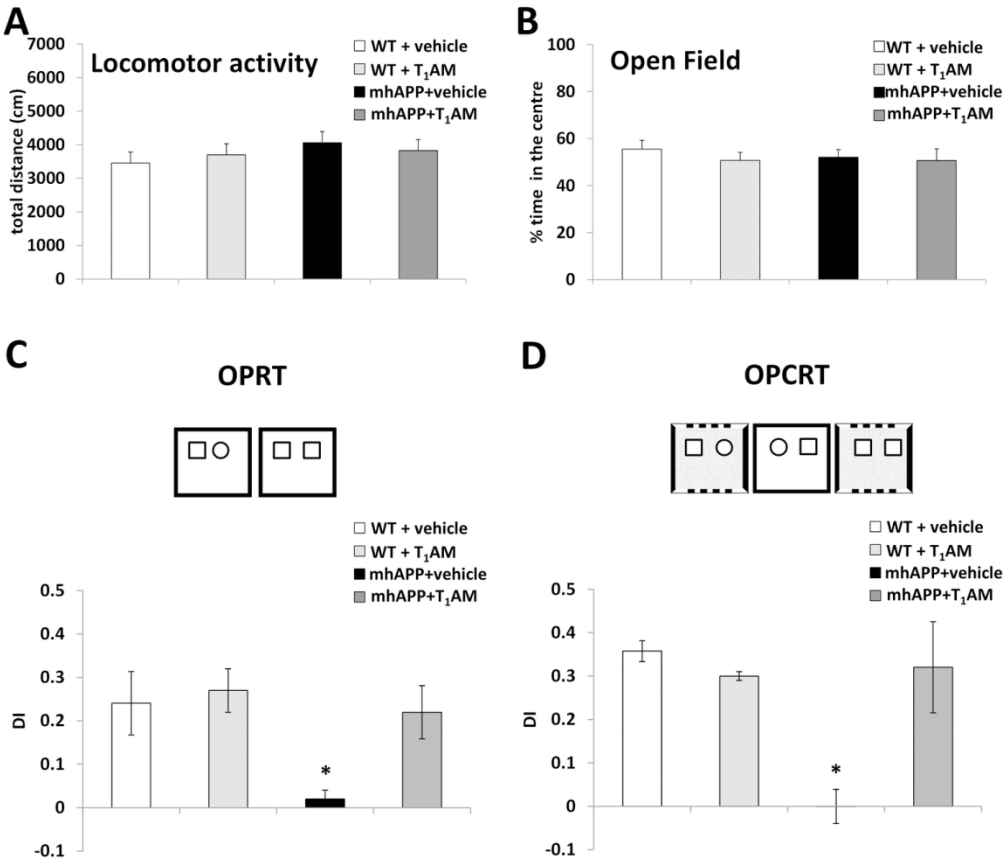
A
Locomotor activity
total distance (cm)
7000
6000
5000
4000
3000
2000
1000
0
WT + vehicle
WT + T1AM
mhAPP+vehicle
mhAPP+T1AM
B
Open Field
% time in the centre
100
80
60
40
20
0
WT + vehicle
WT + T1AM
mhAPP+vehicle
mhAPP+T1AM
C
OPRT
DI
0.5
0.4
0.3
0.2
0.1
0
-0.1
*
WT + vehicle
WT + T1AM
mhAPP+vehicle
mhAPP+T1AM
D
OPCRT
DI
0.5
0.4
0.3
0.2
0.1
0
-0.1
*
WT + vehicle
WT + T1AM
mhAPP+vehicle
mhAPP+T1AM